APPENDIX X
TEMPERATURE EFFETS MODELING DOCUMENTATION

Part I: Barr Consulting's Temperature Effects Modeling Documentation

Part II: The DNR's Temperature Modeling Technical Documentation

Technical Memorandum

To: Joe McGaver, P.E.
From: Ray Wuolo and Rachael Shetka, Barr
Subject: Groundwater Temperature Modeling – Line 5
Date: May 14, 2024
Project: 49161641.00

1   Introduction

This technical memorandum describes the methods and results of modeling the temperature effects of the proposed Line 5 Wisconsin Segment Relocation Project on groundwater beneath streams and wetlands crossed using dry cut-and-cover methods. The pipeline is expected to have temperatures higher than the surrounding soil/geologic deposits and the groundwater in the pore spaces of those deposits for at least portions of the year. The vast majority of streams and tributaries (excluding headwaters tributaries) in the Bad River watershed are "gaining" streams in which the source of baseflow is groundwater discharging into the steams (Leaf et al., 2015). Most wetlands are hydrologically similar to streams in the watershed because both water features are approximately surface expressions of the water table. The main differences between wetlands and streams is that groundwater flow into wetlands is expected to be lower. Therefore, in the assessment of the effects of temperature on streams and wetlands where the pipeline is a few feet below the bed of the stream or wetland, the effects of groundwater flow around the pipeline and into the waterbody/wetland needs to be accounted for in addition to typical heat convection considerations.

The modeling described in the memorandum is not intended to simulate conditions at any one particular crossing. The modeling uses, to the extent feasible, typical hydrologic conditions for stream crossings. The crossing at MP 19.3 of Silver Creek was identified as being the source for typical geologic and hydrologic conditions. This crossing has geotechnical boring data to infer estimates for hydraulic conductivity and storativity/specific storage, stream width and steam flows. Several assumptions needed to be made for model parameters in the absence of site-specific data – these assumptions are described in this memorandum.

2   Conceptual Models

A straightforward conceptual hydrogeologic model was used for the groundwater flow system, illustrated in Figure 1. Groundwater flows at a uniform rate toward the stream, and all groundwater then discharges into the stream upon reaching it. Deep groundwater flow is assumed to not flow into the stream as part of this modeled system. Groundwater flow is horizontal (toward the stream) and becomes vertical near and directly below the stream. The pipeline is assumed to intersect the stream perpendicularly four feet (1.2 m) below the bottom of the stream. The pipeline is approximately parallel to groundwater flow except in the vicinity of the stream, at which groundwater flow is upward and perpendicular to the orientation of the pipeline (i.e., groundwater flows around the pipe). Recharge is assumed to be encapsulated as a component of horizontal groundwater flow and is not explicitly included in the conceptualization. Groundwater flow is assumed to be uniform and steady-state for purposes of this evaluation.

A complimentary conceptual temperature model is illustrated in Figure 2. Sources of thermal input to the model include the pipeline, radiant heat from ambient air at the ground surface, and groundwater flowing

into the model from the model boundaries. The temperature of the pipeline surface varies seasonally, as does air temperature. Groundwater flowing in from the model boundaries is assumed to be approximately equal to average annual air temperature. Air temperature is modeled at the ground surface and is assumed to be 0° C during months when snowpack is present.

3   Numerical Model

The numerical model constructed for this evaluation is designed to be an abstraction of the flow system. It is intended to capture the essential elements of groundwater flow in order to account for the effects of groundwater flowing past the pipeline and into a stream. It is intended to aid in understanding how thermal transfer from the operating pipeline surface may change the temperature of groundwater entering as baseflow into steams, in a scenario typical of the shallow crossings of tributary streams in the Bad River watershed.

The modeling codes used are the codes developed by the USGS: MODFLOW-2005 for groundwater flow, and MT3D for temperature modeling. MT3D is a solute-transport code used in conjunction with MODFLOW. For this evaluation, heat (as represented by temperature) is the "solute" and solute-transport parameters such as diffusion, dispersion, and solid-water partitioning can be treated analogous to a chemical solute because the governing equations describing groundwater solute transport and heat transport have a similar form; therefore, MT3D-USGS may be applied to heat transport problems (e.g., Morway et al., 2023). An alternative approach would be to use the USGS code SEAWAT (Langevin, et al., 2007), which includes additional capabilities to account for changes in density due to changes in groundwater temperature, as well as density-driven flow for differing specific gravity conditions. However, for this evaluation, the added capabilities of SEAWAT are not required.

The numerical model grid is 20 meters by 20 meters, with the highest level of discretization corresponding to the pipeline (trending east-west in model orientation and parallel to groundwater flow) and to the stream (trending north-south in model orientation and parallel to groundwater flow). Vertical discretization consists of 17 layers of variable thickness and a total uniform model thickness of 15 meters. The highest level of vertical discretization (thinnest model layers) ranges from the ground surface to a few meters below the pipeline. Model discretization is shown in Figure 3.

3.1   Flow Parameters and Assumptions

The crossing at MP 19.3 of Silver Creek was identified as being the source for typical geologic and hydrologic conditions for use in this evaluation. The geotechnical boring data available at this location indicates primarily sand in the upper 20 meters. A typical horizontal and vertical value of hydraulic conductivity for sand was assumed: 10 m/day with a vertical anisotropy value of 1/10th horizontal.

None of the borings identify depth to the water table, although driller's logs indicated moist to wet conditions from the ground surface and below. Therefore, the water table was assumed to be at the ground surface for this evaluation. No data were available to estimate hydraulic gradients, so the hydraulic gradient was assumed to be toward and perpendicular to the stream. Boundary conditions and stream stage were assumed such that the horizontal hydraulic gradient is approximately 0.05. This assumed hydraulic gradient of 0.05 is likely on the high side of expected values but allows for simulating temperature exchange between groundwater and the pipeline at a conservatively high value. The steady-state groundwater baseflow contribution in the simulation is 0.0008 cfs per meter of stream length, which is a conservatively low assumption. A north-flowing slope to the stream was estimated from topographic maps for the MP 19.3 area of 0.0025.

The stream is represented by a constant head boundary condition. Groundwater flow from the east and west sides of the model are simulated using constant head boundaries at those model edges and was included only in the lower half of the model layers.

The pipeline was modeled at its approximate thickness and width as a zone of very low hydraulic conductivity of 0.05 m/day.

3.2 Temperature Parameters and Assumptions.

Temperature modeling using MT3D is transient, with temporal variability in air temperature and pipeline temperature. Monthly "stress periods" (modeling time steps in which temperature changes for air and the pipeline are changed in the model) were used. Monthly averages of daily high and low air temperature were obtained from the U.S. Climate Data for Mellon, Wisconsin. The monthly air temperature value was calculated as the average of the mean high and low daily temperature, with the minimum temperature set at $0°$ C if the air temperature was below freezing. The monthly pipeline temperatures were provided by Enbridge for Line 5 for 2023. Monthly air and pipeline temperatures are plotted in Figure 4.

Air temperature boundary conditions were set on top of the model (Layer 1), excluding the stream. The stream temperature varies in the model simulations in response to changes in the groundwater temperature. Air temperature varied monthly. Pipeline temperature was set as a variable concentration boundary within the model and varied monthly. Deep groundwater temperature from bottom layers on the east and west edges of the model was set as a constant value of $11.5°$ C – equal to the average daily temperature at Mellon, Wisconsin. The temperature at all other model cells was computed by the model during simulations, in a range between $0°$ C and $20°$ C.

Solute-transport parameters for temperature applicable to sand are listed in metric units in Table 1.

Table 1 Summary of Solute Transport Parameters for Sand

Parameter	Value	Source
total porosity	0.25	Typical value for sand
bulk thermal conductivity of aquifer	2.395	https://pubs.usgs.gov/tm/tm6a22/pdf/tm6A22.pdf
thermal molecular diffusion coefficient	1.98E-01	https://pubs.usgs.gov/tm/tm6a22/pdf/tm6A22.pdf
thermal distribution factor	1.70E-04	https://pubs.usgs.gov/tm/tm6a22/pdf/tm6A22.pdf
bulk aquifer density	1762.035	Typical value for glacially deposited sand
effective porosity	0.22	Typical value for sand
longitudinal dispersivity	50	Zheng, Chunmiao, and Gordon D. Bennett. Applied contaminant transport modeling. Vol. 2. New York: Wiley-Interscience, 2002.,https://www3.epa.gov/ceampubl/learn2model/part-two/onsite/longdisp.html
transverse horizontal dispersivity	5	Zheng, Chunmiao, and Gordon D. Bennett. *Applied contaminant transport modeling*. Vol. 2. New York: Wiley-Interscience, 2002.
transverse vertical dispersivity	0.5	Zheng, Chunmiao, and Gordon D. Bennett. *Applied contaminant transport modeling*. Vol. 2. New York: Wiley-Interscience, 2002.

3.3   Simulation Approach

The groundwater flow portion of the model is a steady-state simulation. The temperature modeling is a transient simulation with month-long stress periods/time steps as well as substantially smaller time steps withing each stress period. The temperature model consists of (1) a "ramp-up" period of three years in which the air temperature changes monthly but there is not a pipeline thermal source, followed by (2) a three-year period in which the air temperature continues to vary monthly, and the pipeline temperature varies monthly. The ramp-up period was used to ensure that the monthly air temperature effects were well established prior to introducing the pipeline as an additional source of thermal input. For both the air temperature and the pipeline temperature, one year's worth of monthly data was repeated for each successive year (i.e., the same yearly data was assumed for future conditions).

4   Model Results and Discussion

The model results are the calculation of the temperature at various depths throughout the model at any given simulation time, including the temperature of groundwater directly above the pipeline and directly below the stream. The model simulations of groundwater temperatures in profile (along the east-west transect that includes the pipeline) and in plan view (the model layer directly above the pipeline) are

shown in Figures 5 through 10 for the months of January, March, May, July, September, and November. Figure 11 compares the simulated temperature with the present pipeline and in the absence of the pipeline in the model directly above the pipeline and at the midpoint of the stream. Also plotted in Figure 11 is the simulated temperature of groundwater directly above the pipeline but at the bottom of the stream bed. As expected, the temperature of the groundwater flowing into the stream is several degrees lower than the temperature of groundwater directly above the pipeline (particularly in the winter months) because the seasonal fluctuation of air temperature has a much greater effect on shallow groundwater temperatures than does the effects of the pipeline. Figure 12 shows the temperature increase and periods of time when the groundwater temperatures directly above the pipeline (and below the midpoint of the stream) are higher with the pipeline and when they are lower with the pipeline.

The results of the modeling indicate that the pipeline increases the temperature of the groundwater flowing upward around the pipeline by a maximum of approximately 3° C in late fall. Over the course of a year, the average increase in the temperature of the groundwater flowing upward around the pipeline and into the stream is 1.15° C. The modeling predicts that the presence of the pipeline actually decreases the groundwater temperature in May and early June, which is likely due to the pipeline slightly inhibiting flow of warmer groundwater from depth, but this effect is very localized at the pipeline within the model. This 1.15° -3° C range of temperature falls well within the normal temperature variability of the ground and surface water.

To illustrate the localized effect of the increased groundwater temperature resulting from the pipeline on the overall heat flux into the stream, the total modeled heat flux into the 20-meter-long stream segment simulated in the model was calculated with and without the pipeline. This is accomplished by multiplying the temperature by the groundwater flow into the stream (i.e., the baseflow). The heat flux during the highest period of temperature difference (October and early November) without the pipeline is 25.06 C° x m^3/day. The heat flux with the pipeline is 25.08 C° x m^3/day. These results suggest that the change in stream temperature resulting from the pipeline heat flux would likely be difficult, if not impossible to measure. Groundwater temperature variations due to changes in air temperature are significantly greater and more impactful on stream temperature than the effects of the pipeline. These calculations do not take into account the further mixing of water flowing in the stream from upgradient sources, which would further reduce the pipeline's effect on surface-water temperature.

5   Sensitivity Analysis

Simulations were performed for silt and peat in order to evaluate the sensitivity of the modeling results to changes in hydraulic conductivity and the thermal properties of different deposit types that would typically be encountered at streams and wetlands in the watershed. Silt and peat were chosen to compare to the results using parameters for sand. Silt and peat have lower hydraulic conductivity values (i.e., permeability) than sand and will reduce the rate of groundwater flow to the stream and the upward rate of groundwater flow around the pipeline and into the stream. Silt and peat are also more likely to be encountered in slower flowing stream reaches and wetlands.

The thermal properties of silt and peat used in this evaluation are compared to those for sand in Table 2. Silt and sand have similar properties because they are composed mainly of silica and differ primarily in the size of the grains. Peat has more organic material and clay minerals, resulting in somewhat different thermal properties. Porosity is also greater in peat.

Table 2. Model Properties for Sand, Silt, and Peat Used in Sensitivity Analysis

Parameter	Sand	Silt	Peat
total porosity	0.25	.3	.45
bulk thermal conductivity of aquifer	2.395	2.395	0.555
thermal molecular diffusion coefficient	1.98E-01	1.98E-01	1.2E-02
thermal distribution factor	1.70E-04	1.70E-04	4.49E-04
bulk aquifer density	1762.035	1400	1281
effective porosity	0.22	0.22	0.45
longitudinal dispersivity	50	50	50
transverse horizontal dispersivity	5	5	5
transverse vertical dispersivity	0.5	0.5	0.5
Hydraulic conductivity - horizontal (m/d)	10	1	0.3
Hydraulic conductivity – vertical isotropic coefficient	0.1	0.1	1

The results of the sensitivity analysis are shown in Figure 13. Figure 13 compares the simulated temperatures directly above the pipeline for sand, silt, and peat and compares these results to the simulation with sand and no pipeline. The overall differences between the three deposit types are not great. Thermal and hydrologic parameters for sand are predicted to result in higher temperatures for shallow groundwater than silt or peat (which behave very similarly). Groundwater temperatures for silt and Peat are predicted to be more affected by changes in air temperature than sand. These differences are most likely attributable to the higher permeability of sand and its ability to conduct deeper groundwater past the pipeline. Accordingly, the model results in Section 4 above (addressing sand) represent the greatest temperature change to groundwater expected from pipeline operations, as compared to other

soil conditions. As noted above, this 1.15° -3° C range of increase in temperature falls well within the normal temperature variability of the ground and surface water.

6   Summary and Conclusions

Utilizing USGS modeling codes a numerical model was constructed to examine the effects of the proposed Line 5 Relocation Segment on temperature at stream crossings where the pipeline is approximately four feet below the bottom of the stream bed. In the absence of site-specific data, conditions typical of crossings in the area were used. Variations in pipeline temperature and air temperature were incorporated for a year-long period. Groundwater flow was assumed to be toward the stream and groundwater discharges into the stream. The effect of groundwater flowing around the pipeline and into the stream (advection) was examined. Conduction and heat exchange between the groundwater and soil was simulated with solute transport parameter values typically used in temperature modeling of groundwater. A sensitivity analysis was performed to compare the results with those for silt and peat deposits.

The pipeline was found to minimally increase the temperature of the groundwater between the top of the pipeline and the bottom of the stream. The temperature of groundwater directly below the stream bed is lower than the temperature of groundwater directly above the pipeline. Groundwater flow around the pipeline and into the stream conducts heat effects (as measured by temperature) into the stream. The heating effects were found to be highly localized to the pipeline and would likely not be measurable in the stream. In contrast, the temporal variations in air temperature were found to have a much greater effect on groundwater temperatures and heat flow into the stream. These calculations do not take into account the further mixing of water flowing in the stream from upgradient sources, which would further reduce the any effect on surface-water temperature. For wetland areas with the water table at or near the ground surface, the effect of air temperature similarly would be significantly greater and more impactful on surface-water temperature than the effects of the pipeline.

7   References

Langevin, C.D., Thorne, D.T., Jr., Dausman, A.M., Sukop, M.C., and Guo, Weixing, 2007, SEAWAT Version 4: A Computer Program for Simulation of Multi-Species Solute and Heat Transport: U.S. Geological Survey Techniques and Methods Book 6, Chapter A22, 39 p., https://doi.org/10.3133/tm6A22

Leaf, A.T., Fienen, M.N., Hunt, R.J., and Buchwald, C.A., 2015, Groundwater/Surface-Water Interactions in the Bad River Watershed, Wisconsin: U.S. Geological Survey Scientific Investigations Report 2015–5162, 110 p., http://dx.doi.org/10.3133/sir20155162.

Morway, E., Feinstein, D.T., and Hunt, R.J., 2023, MODFLOW-NWT, MT3D-USGS, and VS2DH models of 6 hypothetical 1-dimensional variably saturated systems to demonstrate the accuracy of new heat transport capabilities in MT3D-USGS.
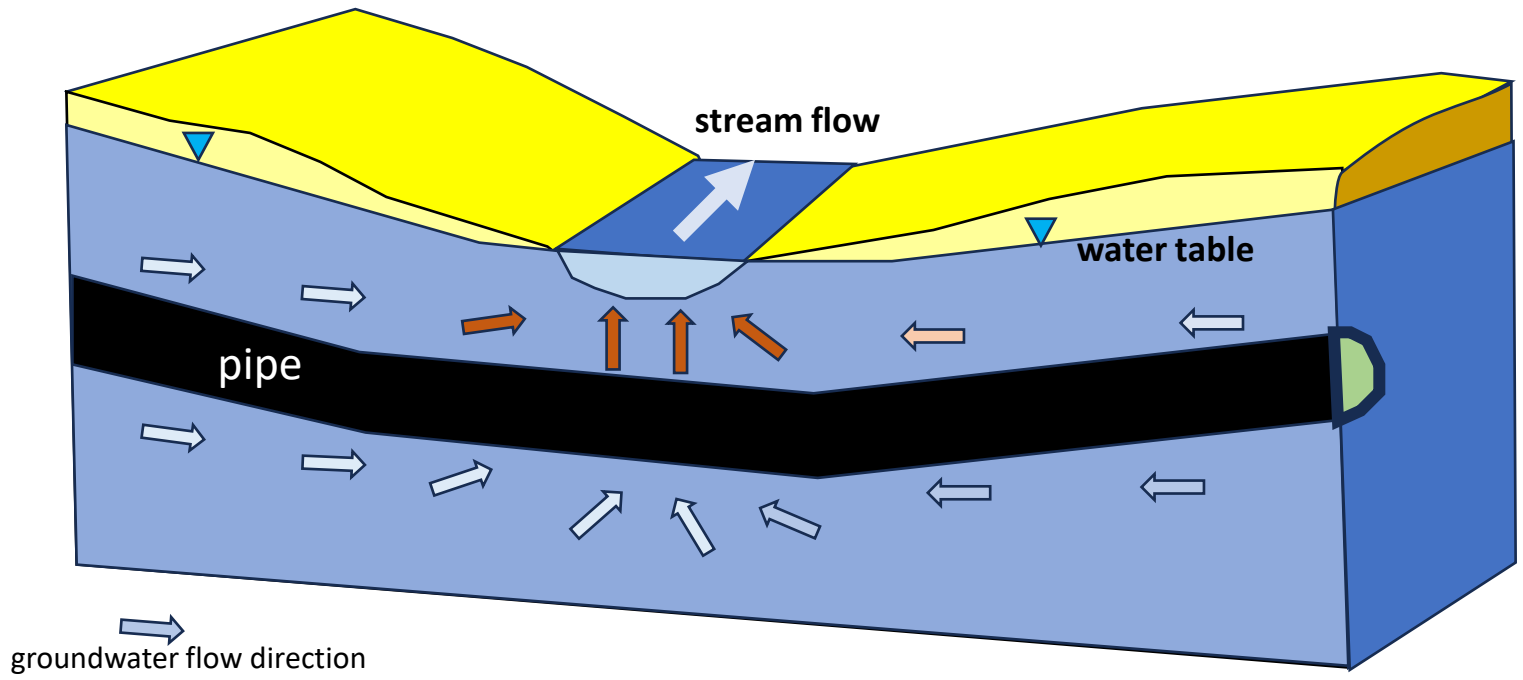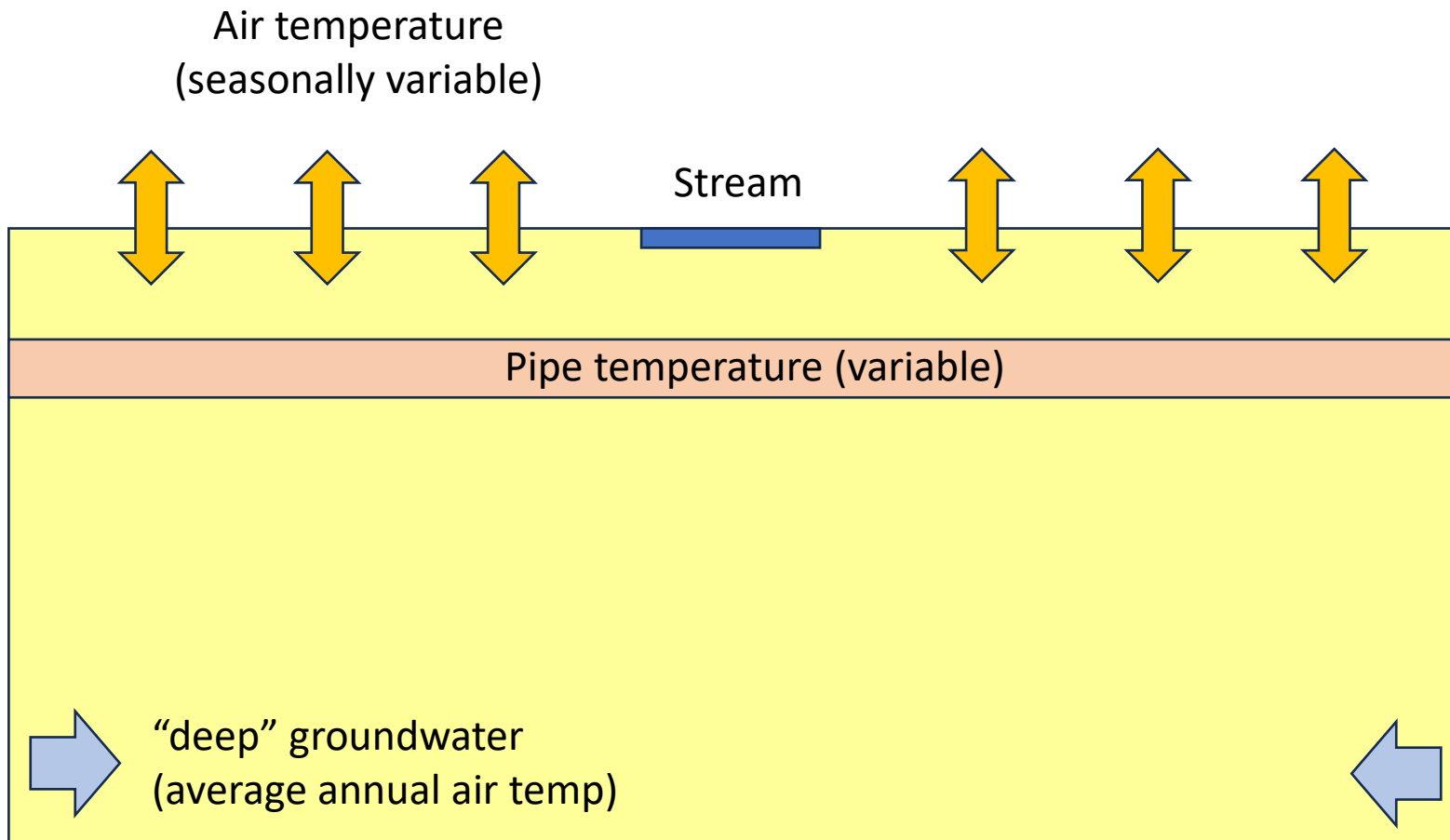
stream flow

water table

pipe

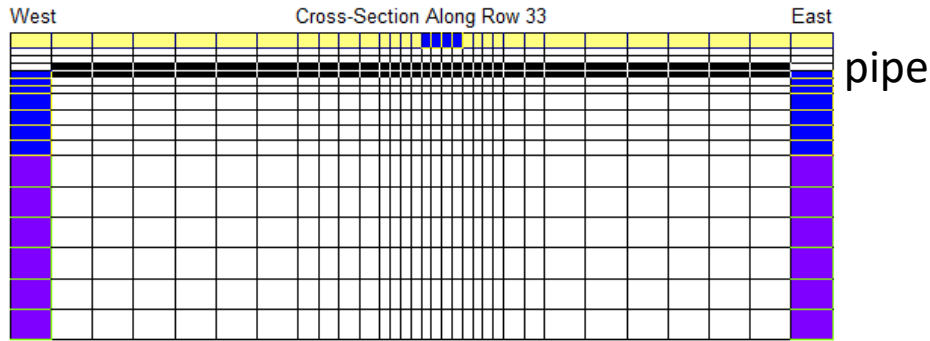groundwater flow direction

Figure 1
Groundwater Flow
Conceptual Model

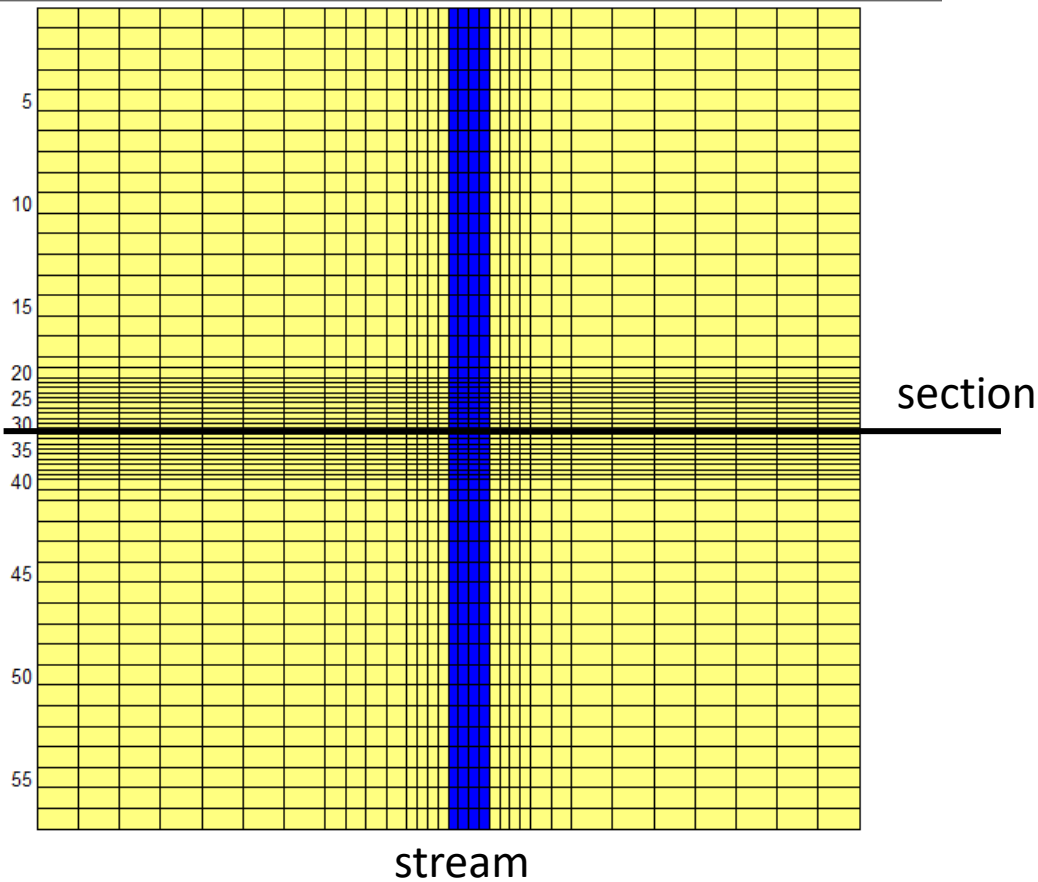Air temperature (seasonally variable)

Stream

Pipe temperature (variable)

"deep" groundwater (average annual air temp)

Figure 2
Temperature
Conceptual Model

West   Cross-Section Along Row 33   East

pipe

Section View

section

Plan View

stream

Figure 3
Model Discretization
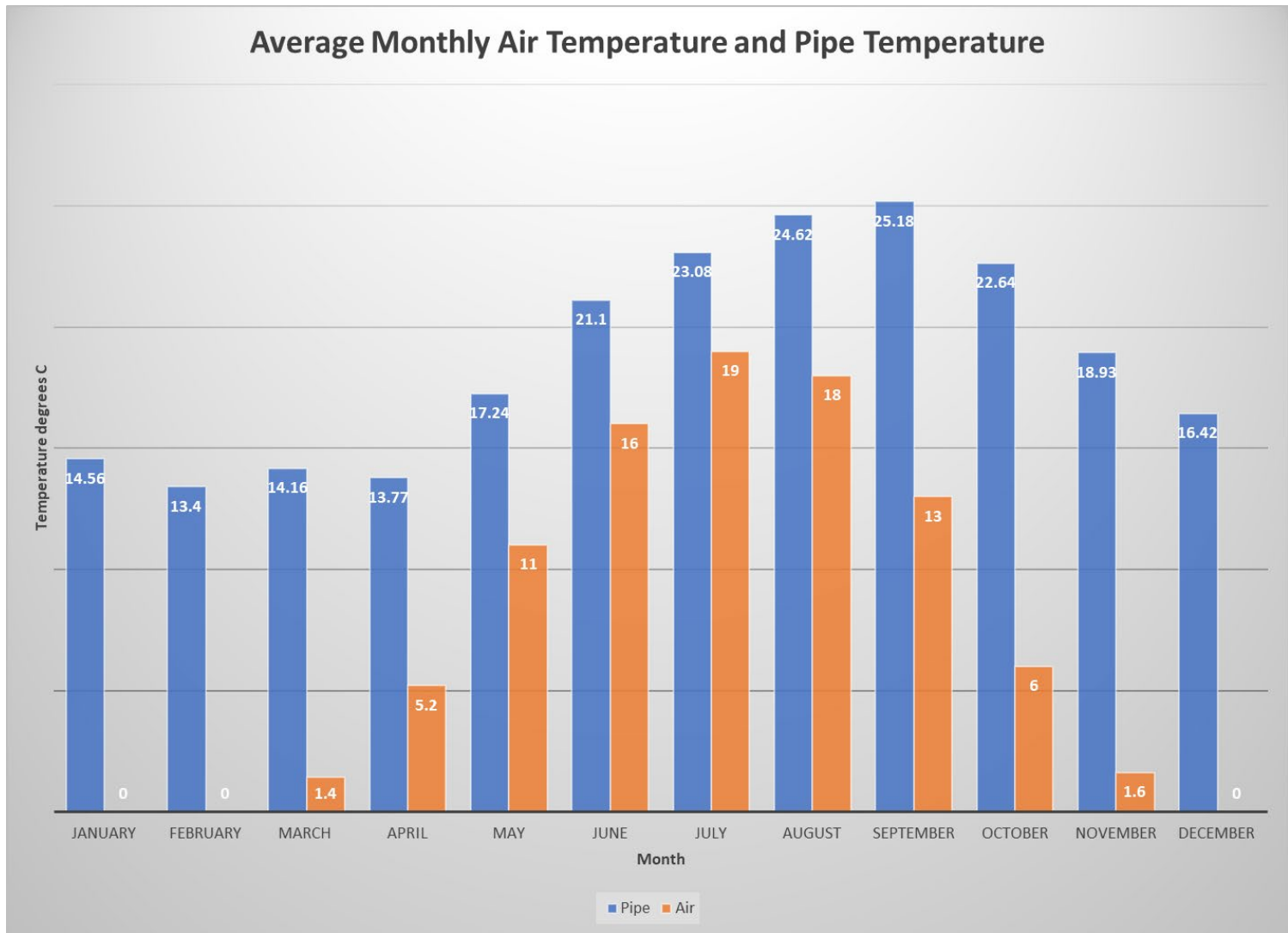
Figure 4
Monthly Air and Pipe
Temperature (Celsius)

15 m

PROFILE ON
SECTION

0 m

pipeline

JANUARY

Simulated Temperature
(Celsius)

16.00

12.00

8.00

4.00

0.20

PLAN VIEW
(layer directly
above pipeline)

section

(arrow vectors show direction of
groundwater flow)
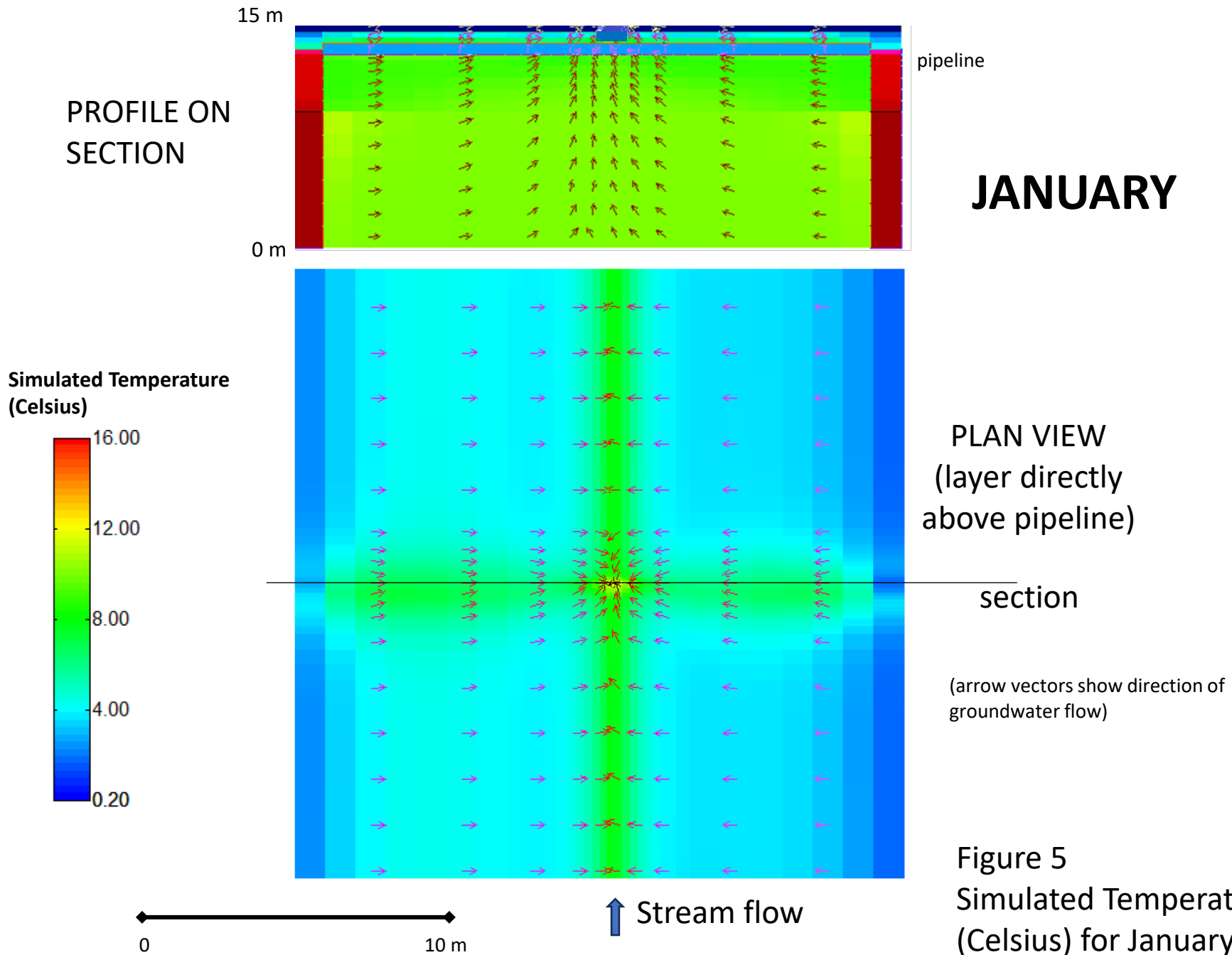
Figure 5
Simulated Temperature
(Celsius) for January

Stream flow

0   10 m

15 m

West   Cross-Section Along Row 33   East

pipeline

PROFILE ON
SECTION

MARCH

0 m

Simulated Temperature
(Celsius)

16.00

12.00

8.00

4.00

0.20

PLAN VIEW
(layer directly
above pipeline)

section

(arrow vectors show direction of
groundwater flow)

0   10 m

↑ Stream flow
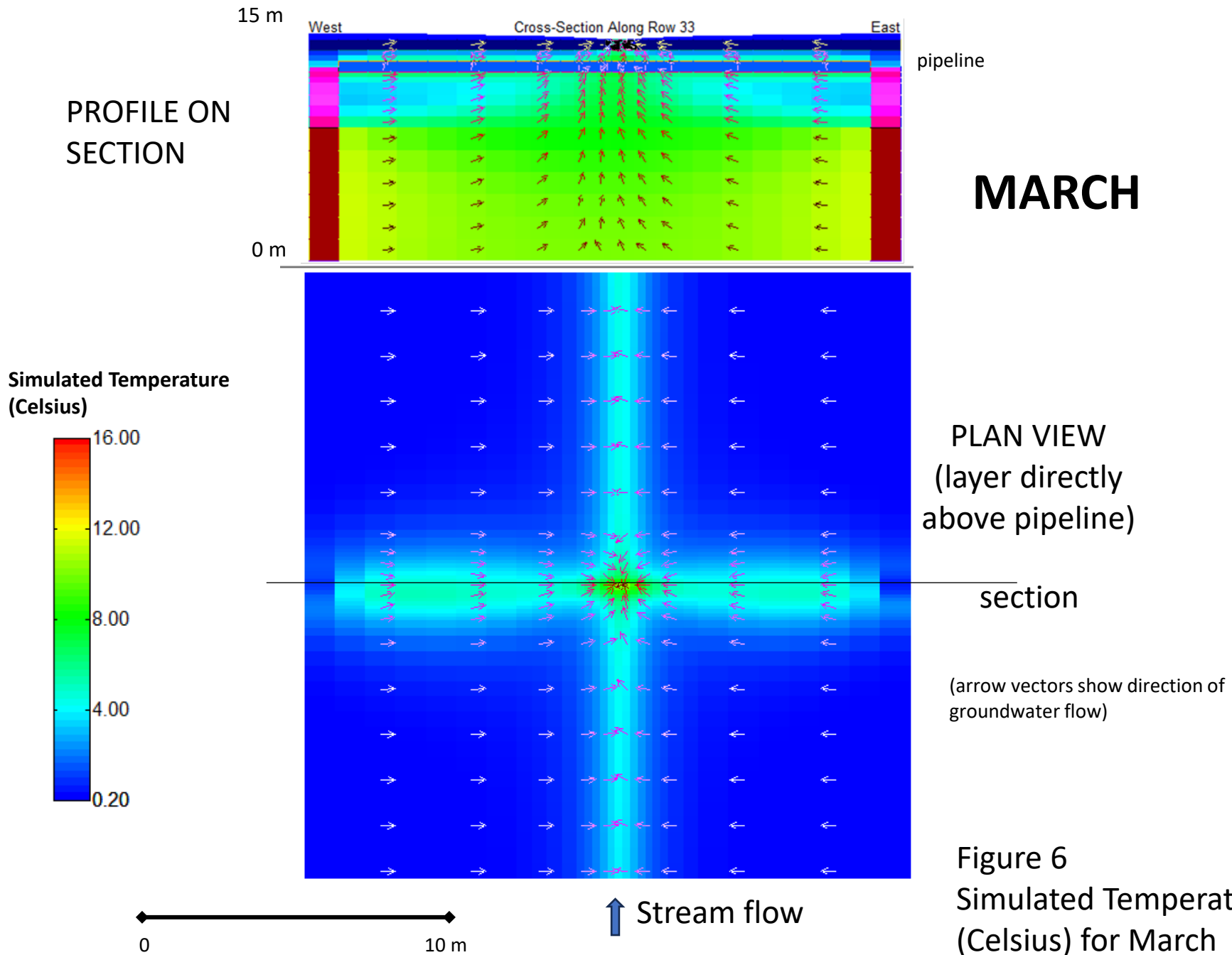
Figure 6
Simulated Temperature
(Celsius) for March

15 m

West — Cross-Section Along Row 33 — East

PROFILE ON SECTION

pipeline

MAY

0 m

Simulated Temperature (Celsius)

16.00

12.00

8.00

4.00

0.20

PLAN VIEW (layer directly above pipeline)

section

(arrow vectors show direction of groundwater flow)

↑ Stream flow
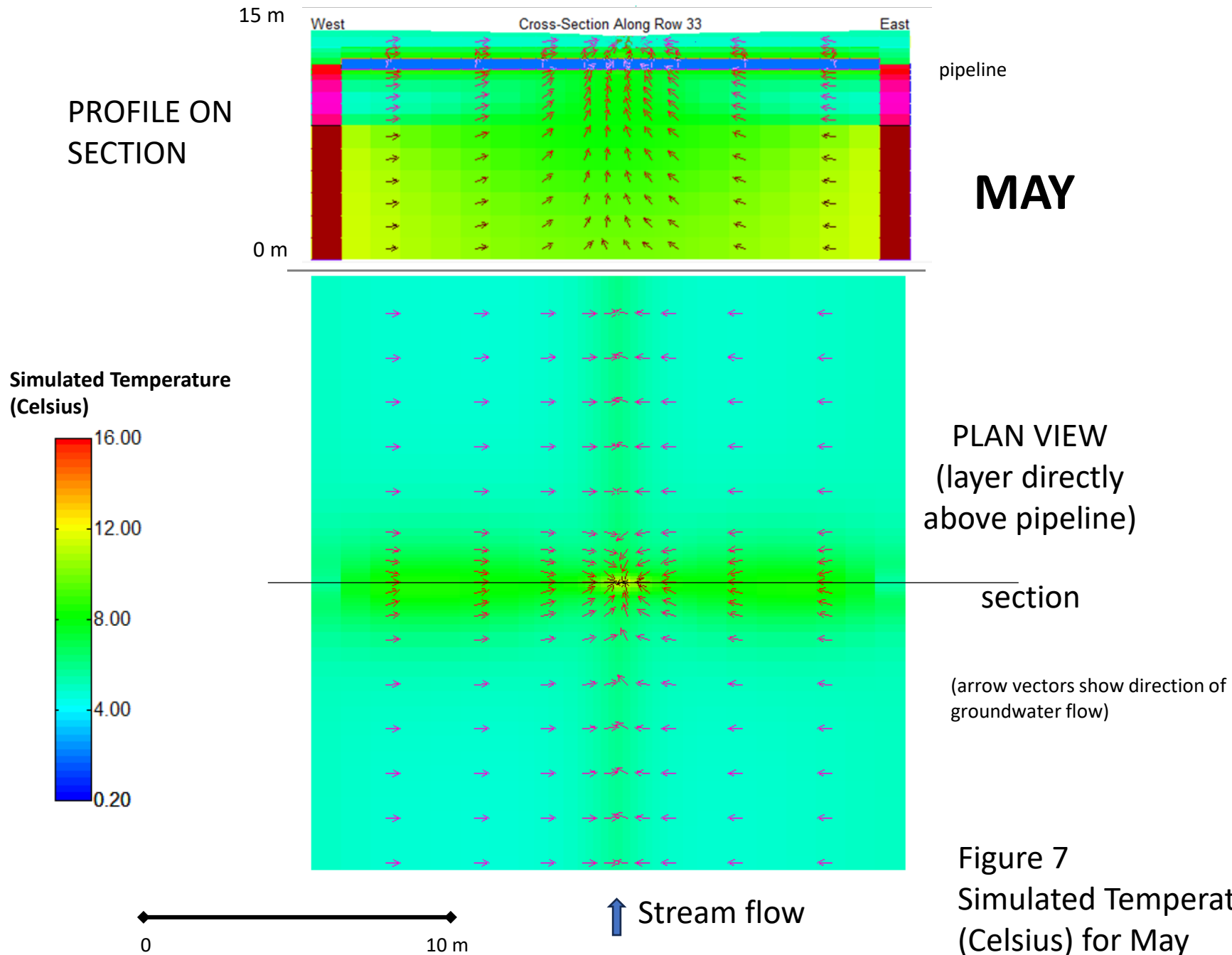
Figure 7
Simulated Temperature (Celsius) for May

0   10 m

15 m

West — Cross-Section Along Row 33 — East

pipeline

PROFILE ON SECTION

0 m

JULY

Simulated Temperature (Celsius)

16.00

12.00

8.00

4.00

0.20

PLAN VIEW
(layer directly above pipeline)

section

(arrow vectors show direction of groundwater flow)

0   10 m

↑ Stream flow
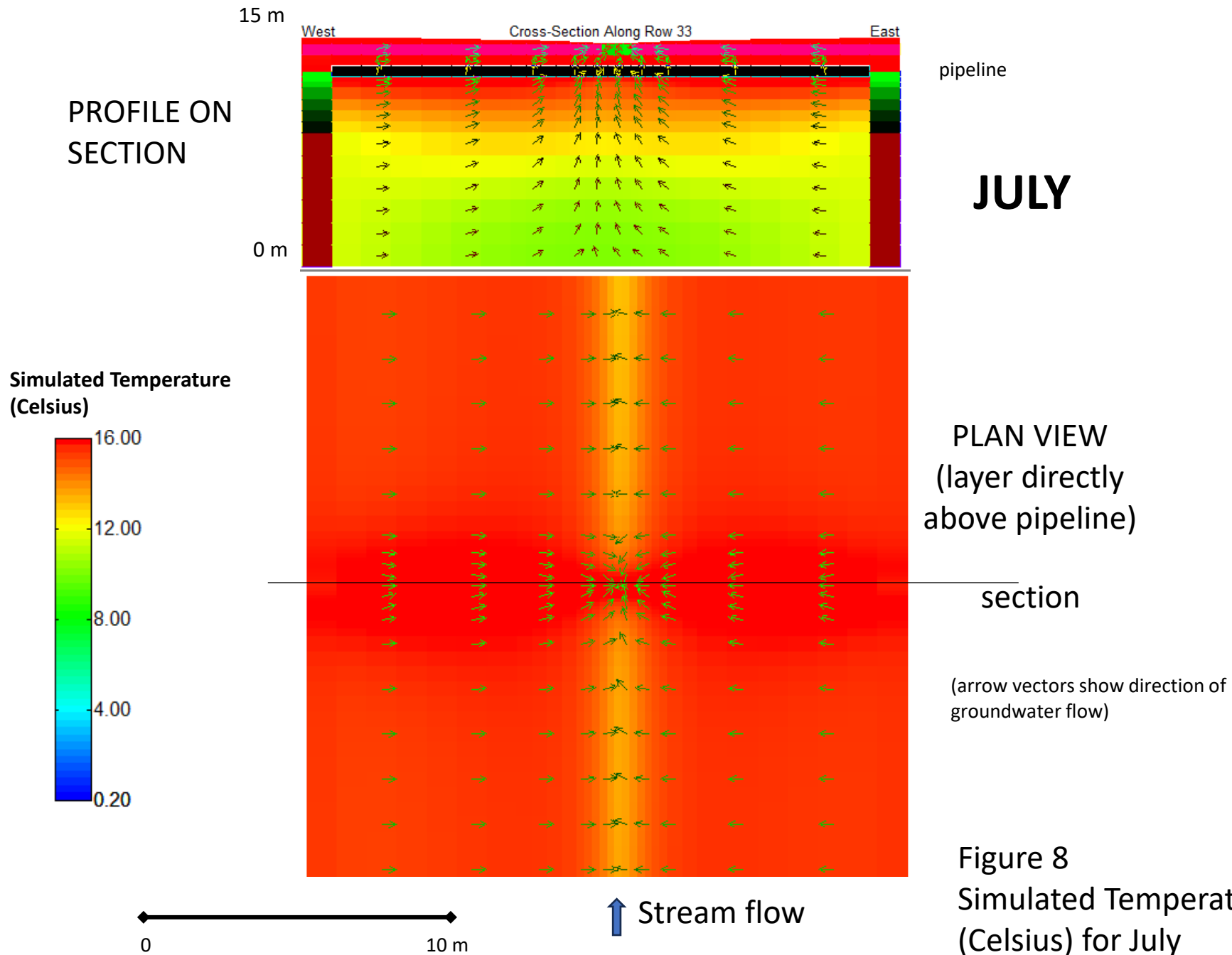
Figure 8
Simulated Temperature (Celsius) for July

15 m

West   Cross-Section Along Row 33   East

pipeline

PROFILE ON
SECTION

SEPTEMBER

0 m

Simulated Temperature
(Celsius)

16.00

12.00

8.00

4.00

0.20

PLAN VIEW
(layer directly
above pipeline)

section

(arrow vectors show direction of
groundwater flow)
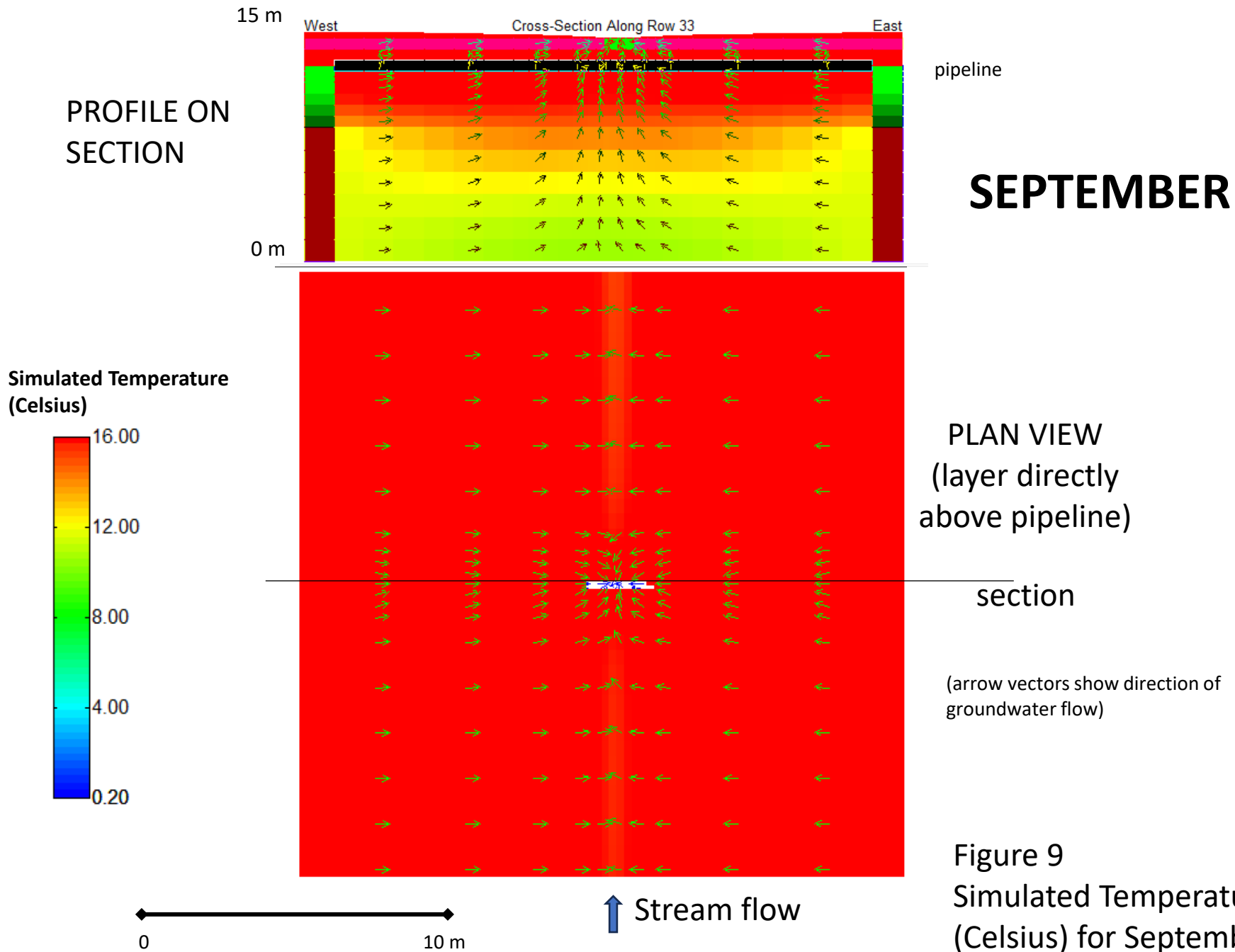
Figure 9
Simulated Temperature
(Celsius) for September

0   10 m

Stream flow

15 m

West   Cross-Section Along Row 33   East

pipeline

PROFILE ON SECTION

0 m

NOVEMBER

Simulated Temperature (Celsius)

16.00

12.00

8.00

4.00

0.20

PLAN VIEW (layer directly above pipeline)

section

(arrow vectors show direction of groundwater flow)
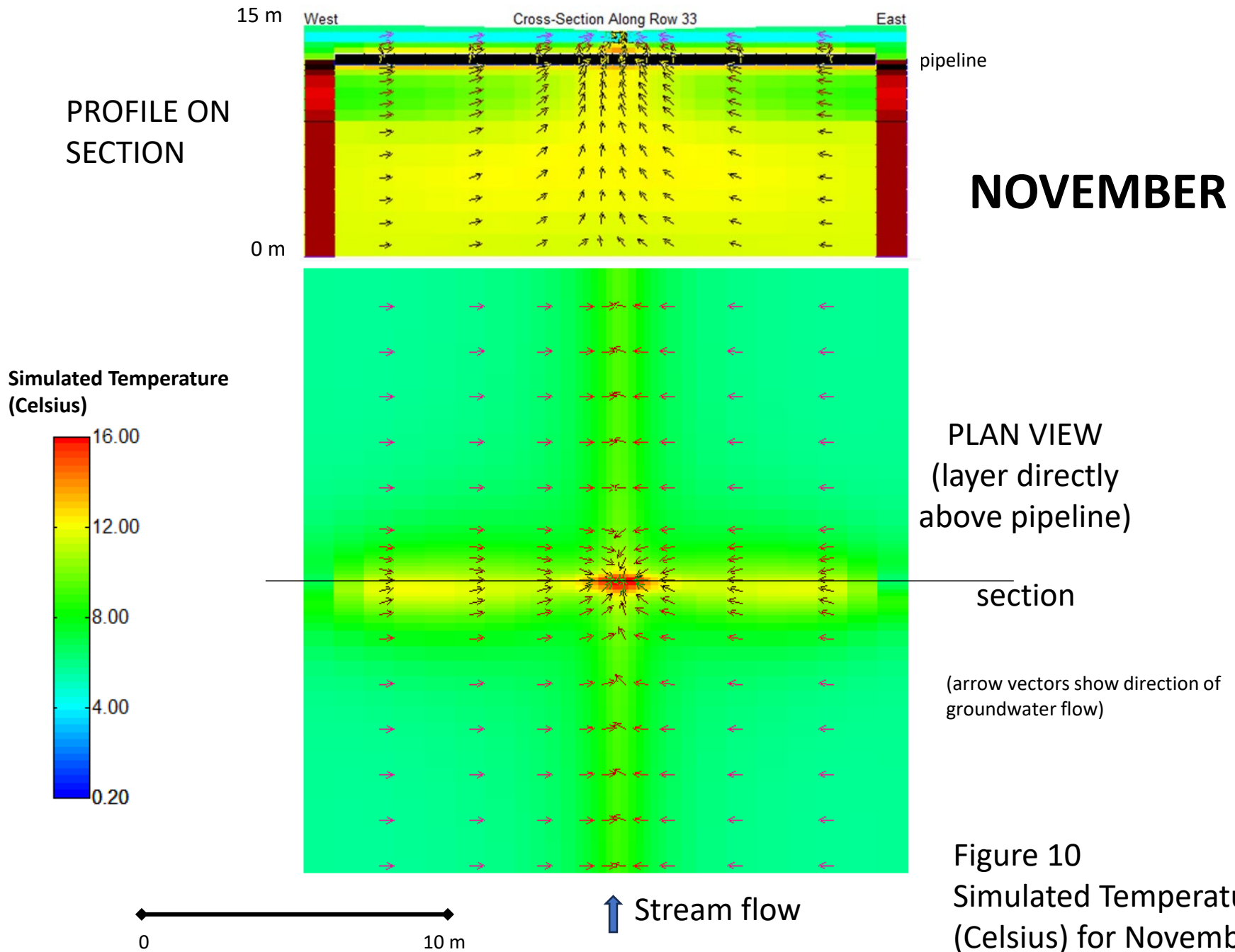
Figure 10
Simulated Temperature (Celsius) for November

↑ Stream flow
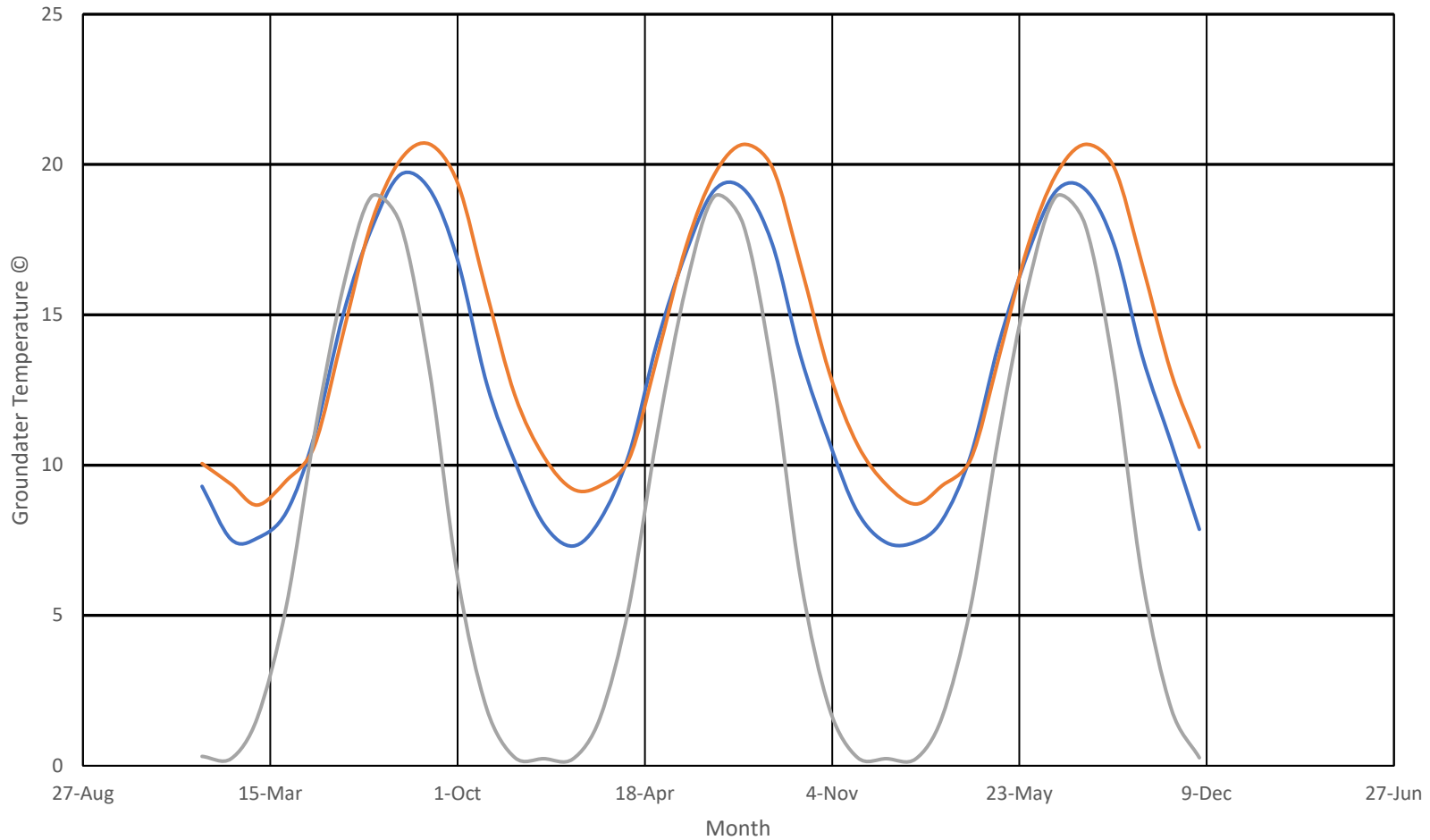
0   10 m

Figure 11
Simulated Temperature (Celsius) in the Model Layer directly
Above the Pipe and Below the Mid-Point of the Stream With
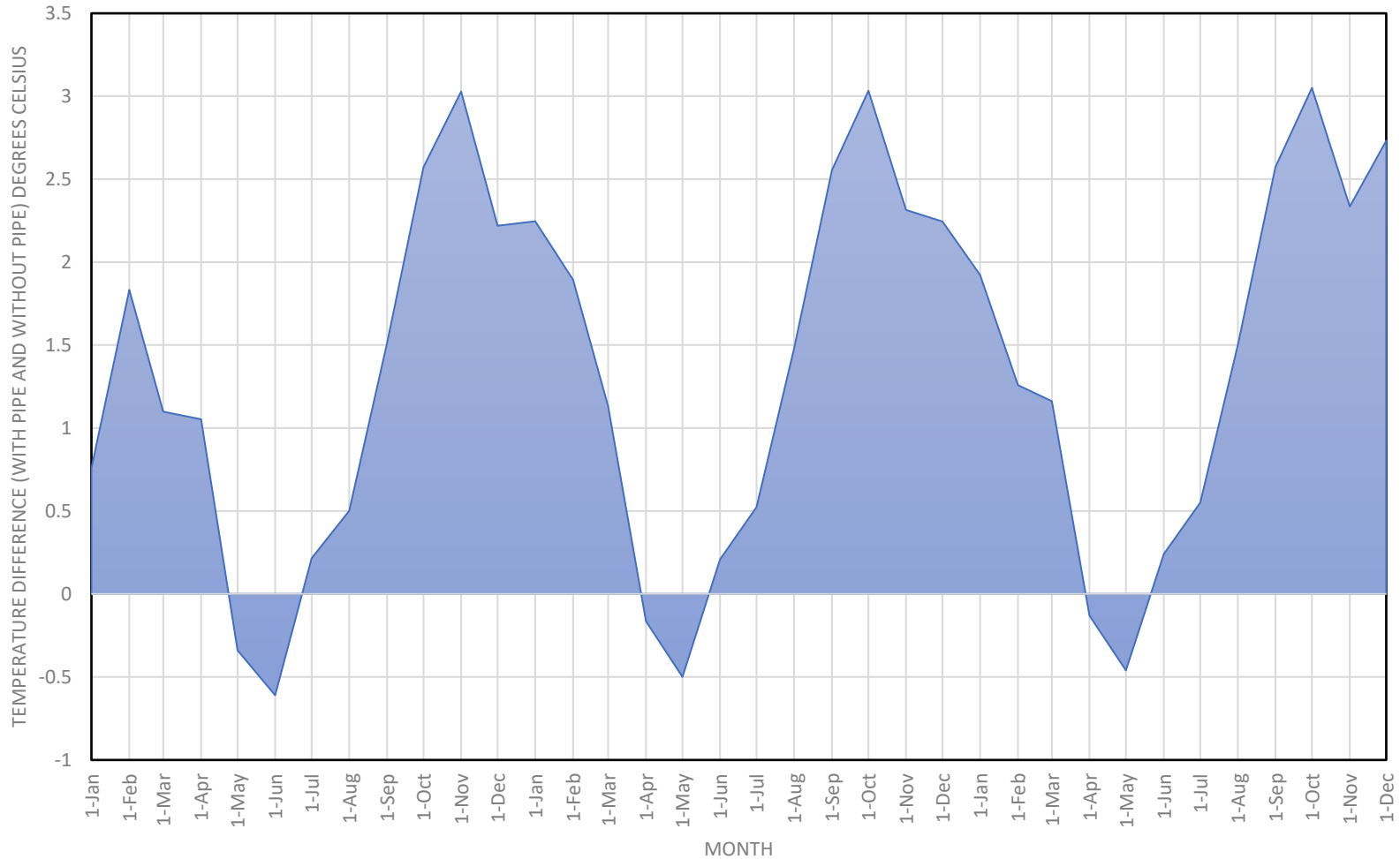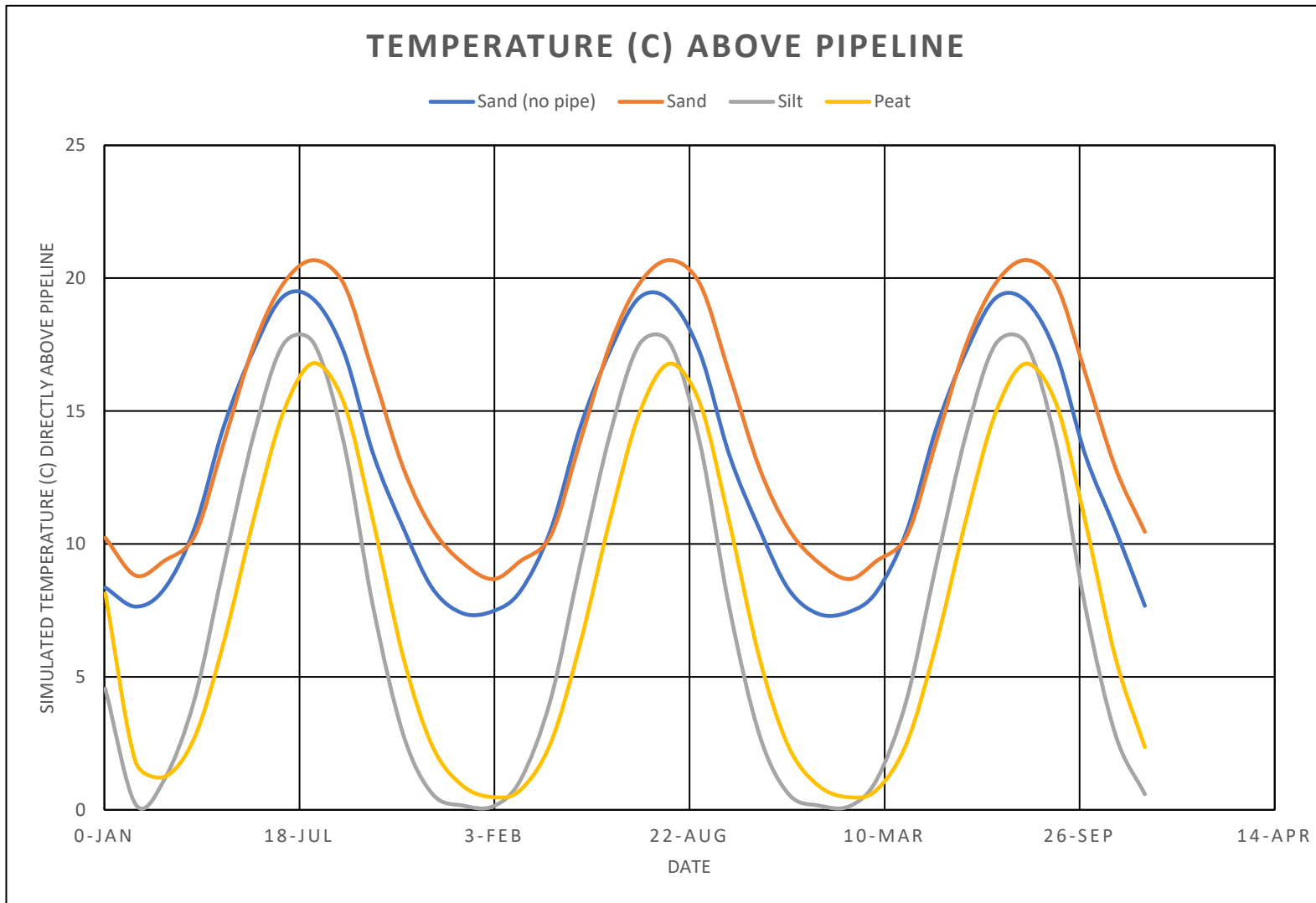and Without the Pipe

Figure 12
Simulated Difference in Temperature (Celsius) in the
Model Layer directly Above the Pipe and Below the
Mid-Point of the Stream With and Without the Pipe

Figure 13
Results of Sensitivity Analysis for Thermal
Properties: Comparison of Results for Sand, Silt, and
Peat.

1 Introduction

DNR conducted temperature modeling to quantify the potential for clearing associated with pipeline to increase stream temperatures.

2 Modeling Approach

The main approach used is based on a 1-dimensional, steady-state heat transfer model. This model is well-suited for first-order approximations of impact in certain scenarios. Heat transfer and evapotranspiration dyanmics are considered after the approach used in Dingman (2003). The approach quantifies evapotranspiration and head transfer using the equation

$$\lambda E = K + L - G - H + A_w - \frac{\Delta U}{\Delta t}$$

where λE is the latent heat exchange, K is net shortwave radiation, L is net longwave radiation, G is net output via downward conduction from the water surface, H is is the output of sensible-heat exchange with the atmosphere, A_w is the advective heat flow through the system. ΔU si the change in the amount of heat storage per unit area and Δt is the timestep over which this heat storage changes.

By rearrangement, this equation becomes:

$$\Delta U = \Delta t(K + L - G - H + A_w - \lambda E)$$

which solves for the change in energy based on how the other values evolve with time. Our assumption of complete mixing of the water column (and negligible exchange with the streambed in comparison to advection) leads to cancellation of the G term such that the final equation is

$$\Delta U = \Delta t(K + L - H + A_w - \lambda E)$$

or, alternatively,

$$\frac{\mathrm{d}U}{\mathrm{d}t} = K + L - H + A_w - \lambda E$$

making the final function $U(t)$

$$U(t) = \int K + L - H + A_w - \lambda E \, \mathrm{d}t$$

2.1 Shortwave Radiation

Shortwave radiation input is sourced from NOAA and is a typical value for a clear-sky day in July at the latitude and longitude of the project area. Clear-sky shortwave radiation is well-modeled empirically in general but was not explicitly modeled for the purposes of this exercise because the timescale over which effects occur is not sufficient for changing solar radiation with time to matter in most cases. Shortwave radiation is reported in units of $\mathrm{J\,m^{-2}\,s^{-1}}$ (i.e., $\mathrm{W\,m^{-2}}$). The value was adjusted by albedo (a) which is the reflectivity of the surface hit by radiation. This adjusts the final formula:

$$K = K_{\mathrm{in}} \cdot (1 - a)$$

in this case, albedo is assumed to be between 0.05 and 0.1.

2.2 longwave radiation

Longwave radiation is basically heat energy on the electromagnetic spectrum and is modeled using the following equations:

$$L_{\text{net}} = L_{\text{in}} - L_{\text{out}}$$

where L_{in} is modeled as:

$$L_{\text{in}} = 2.7 \cdot P_{\text{vap}} + 0.245 * T - 45.14$$

where P_{vap} is vapor pressure and T is temperature in kelvin. This equation returns a value in units of $\text{MJ}\,\text{m}^{-2}\,\text{d}^{-1}$ which is then converted by subsequent equations into the final heat flux value in $\text{J}\,\text{m}^{-2}\,\text{s}^{-1}$.

Outgoing radiation is modeled by:

$$L_{\text{out}} = \left(\varepsilon_{\text{water}} \cdot \sigma_{\text{sb}} \cdot \mathcal{T}^4\right) + (1 - \varepsilon_{\text{water}}) \cdot L_{\text{in}}$$

which is the black-box radiation of the water. $\varepsilon_{\text{water}}$ is the emissivity of water (the reciprocal of albedo), σ_{sb} is the stefan-boltzmann constant, and $\mathcal{T}$ is the temperature in units of Kelvin.

2.3 Heat Advection

Heat advection is given by

$$A_w = c_w \cdot \rho_w \cdot \left(P \cdot T_P + Q_i \cdot T_{Q_{\text{in}}} - Q_{\text{out}} \cdot T_{Q_{\text{out}}} + GW_{\text{in}} \cdot T_{GW_{\text{in}}} - GW_{\text{out}} \cdot T_{GW_{\text{out}}}\right)$$

which is the mass balance of the water balance terms in the equation (Precipitation P, groundwater GW, Discharge Q) multiplied by their temperature. Most terms in this equation, for the purposes of this analysis, were neglected:

$$A_w = c_w \cdot \rho_w \cdot \left(\cancel{P \cdot T_P} + Q_{\text{in}} \cdot T_{Q_{\text{in}}} - Q_{\text{out}} \cdot T_{Q_{\text{out}}} + \cancel{GW_{\text{in}} \cdot T_{GW_{\text{in}}} - GW_{\text{out}} \cdot T_{GW_{\text{out}}}}\right)$$

Additionally, because of the assumption of steady state, $Q_{\text{in}} = Q_{\text{out}} = Q$, so the equation reduces finally to

$$A_w = c_w \cdot \rho_w \cdot Q \cdot T_Q$$

where c_w is the heat capacity of water, ρ_w is the density of water, Q is the discharge of water, and T_Q is the temperature of the discharge.

2.4 Latent Heat Exchange

Latent heat exchange (λE) is defined form the equation:

$$\lambda E = \lambda_v \cdot \rho_w \cdot E$$

where E is the evaporation rate and λ_v is the latent heat of vaporization for water. Latent heat of vaporization is temperature dependent and equates to

$$\lambda_v = 2501 - 0.00236 \cdot T_s$$

where λ_v is in units of $\text{MJ}\,\text{kg}^{-1}$ and T_s is surface temperature in ℃.

2.5 Evaporation Rate

Evaporation rate is determined by the equation

$$E = \left(-\frac{0.622 \cdot \rho_a}{p \cdot \rho_w}\right) \cdot \frac{\kappa^2 \cdot [u(z_2) - u(z_1)] \cdot [e(z_2) - e(z_1)]}{\left[\ln\left(\frac{z_2 - z_d}{z_1 - z_d}\right)\right]^2}$$

where ρ_a is the density of air, p is atmospheric pressure, ρ_w is water density, $u(z)$ describes the air velocity at elevation z, and $e(z)$ defines the vapor pressure at elevation z. The equation is modified for one elevation vs. surface measurement to

$$E = \left(-\frac{0.622 \cdot \rho_a}{p \cdot \rho_w}\right) \cdot \frac{u(z_m) \cdot [e_s^* - e(z_m)]}{\left[\ln\left(\frac{z_m - z_d}{z_0}\right)\right]^2}$$

oftentimes, the preceding is rearranged with a constant for conceptual simplicity, such that

$$K_E \equiv \frac{0.622 \cdot \kappa^2 \cdot \rho_a}{\rho_w \cdot p \cdot \left[\ln\left(\frac{z_m - z_d}{z_0}\right)\right]^2}$$

so that the evaporation equation becomes

$$E = K_E \cdot u(z_m) \cdot [e_s^* - e(z_m)]$$

the vapor pressures are determined by the equation:

$$e(z) = RH(z) \cdot e^*[T(z)]$$

where RH is relative humidity at elevation z and $e^*[T(z)]$ is the saturation vapor pressure at the tmperature of elevation z. Relative humidity is assumed constant for the purpose of the exercise.

saturation vapor pressure is determined by the equation:

$$e^*(T) = 0.611 \cdot \exp\left(\frac{17.3 \cdot T}{T + 237.3}\right)$$

with T in ℃.

Velocity is assessed with the Prandtl-von Kármán universal velocity distribution, which is:

$$u(z) = \frac{1}{\kappa} \cdot u_* \cdot \ln\left(\frac{z - z_d}{z_0}\right), z_d + z_0 \leq z$$

where $u(z)$ is time-average wind velocity at elevation z, u_* is the friction velocity (an empirical value), κ is a constant, z_d is zero-plane displacment height, and z_0 is roughness height.

2.6 Sensible Heat Exchange

3 Technical implementation

DNR formulated the equations in Section 2 using MATLAB®. Each atomic component was composed into larger formulations with unit conversions where necessary to ensure consistent units. Per-step model outputs were integrated using a discrete forward integration scheme to determine the total temperature gain from the change in storage over time. The model was then run in parallel at small timestep integrity to estimate temperature.

3.1 Data sources

Some values were assumed; for example, relative humidity was assumed as 80% for all scenarios, and air pressure was assumed to be atmospheric (101.325 kPa), air temperature was assumed to be 25℃,

the roughness element height was assumed to be one m, relative humidity was assumed to be 90%, and air velocity was assumed to be 0.3 m s^{-1}.

Observed values came from Enbridge's sampling campaign in September of 2023; observed values included channel width and depth, as well as flow velocity and water temperature. Travel distance was assumed based on the geometery of the right of way.

4 Limitations

This approach's assumption of 1-d heat flow with constant velocity will tend to elide the details of the actual heat distribution in a stream. For example, shading from vegetation, evapotranspiration from the surrounding landscape, and unequal velocities at different reaches and different times of year will tend to change the actual value of heat increase (or loss) over time and space. The assumptions in this modeling exercise are designed to represent the worst-case for heat transfer from clearing, with the implicit counterfactual of no heat increase over the crossing span.

5 Outputs

Outputs for all model runs are shown in Table 1. Figure 1 shows the distribution of heat outputs, which are typically on the order of a few hundredths of a degree celsius of temperature increase based on the water velocity observations and temperature differences.
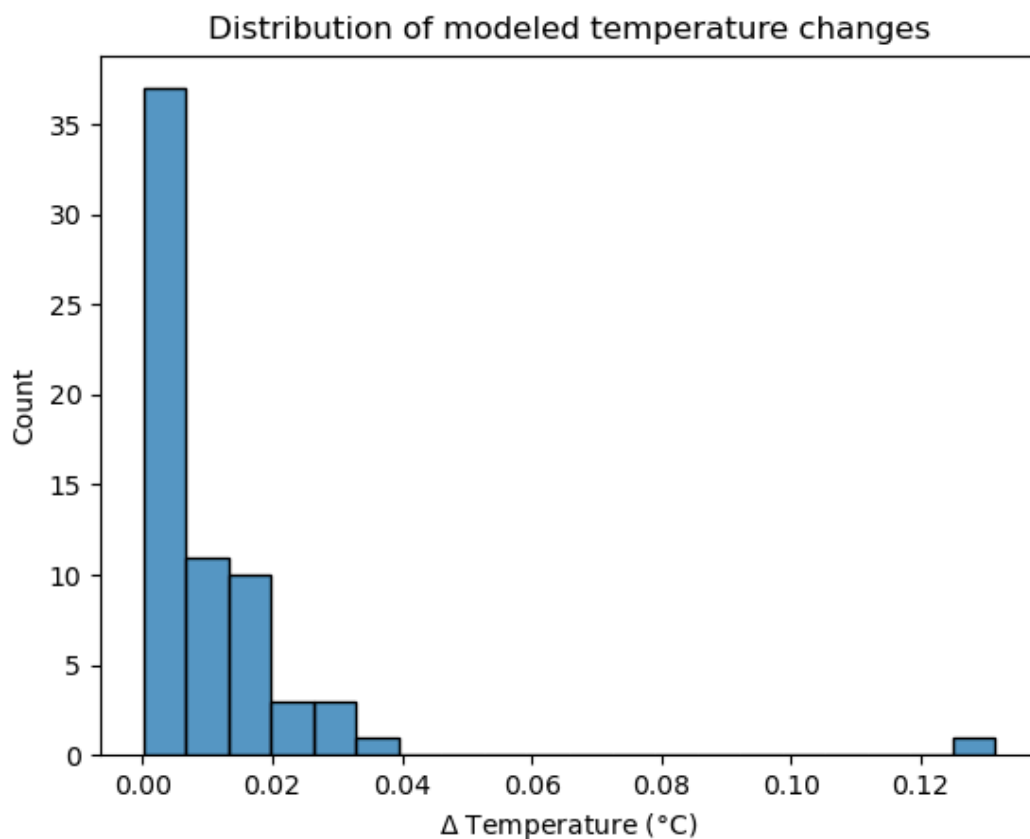

Figure 1: Histogram of changes in temperature from modeled data inputs

Table 1: Modeled Heat increase due to clearing from ROW construction based on 1-d Temperature modeling for crossings with sampled temperature data for September, 2023.

Site ID	Channel Depth m	Channel Width m	Channel Velocity m s^{-1}	Temperature °C	Δ Temperature °C
sasa004p	0.091	0.914	0.018	14.2	0.0035
sasa020i	0.114	3.353	0.063	15	0.0097
sasa066i	0.328	4.267	0.061	16.9	0.0033
sasa070e	0.122	1.219	0.003	15	0.0003
sasa071p	0.168	3.825	0.116	14.5	0.0123
sasa071p_x	0.152	3.048	0.155	14.5	0.0183
sasa1005p	0.533	11.887	0.469	17.3	0.0157
sasb006p	0.762	11.125	0.184	16.15	0.0043
sasb1007e	0.101	1.829	0.003	14.7	0.0004
sasc022p	0.127	3.658	0.212	14	0.0301
sasc025i	0.648	1.448	0.003	13.8	0.0001
sasc031i	0.061	1.219	0.061	14	0.0178
sasc039i	0.152	5.791	0.035	15.95	0.004
sasc041p	0.21	3.429	0.026	16.45	0.0021
sasc1003p	0.076	1.996	0.024	16.1	0.0056
sasc1006p	0.137	0.991	0.04	15	0.0051
sasc1010i	0.122	1.097	0.006	14.55	0.0007
sasc1012p	0.183	5.182	0.392	16.4	0.0384
sasc1014p_x1	0.198	2.515	0.012	14.9	0.001
sasc1014p_x2	0.152	1.219	0.024	15.4	0.0028
sasd011p	0.191	2.134	0.123	15.5	0.0116
sasd015i	0.164	1.6	0.037	15.6	0.0039
sasd1011p_x1	0.366	3.048	0.076	15	0.0037
sasd1011p_x2	0.305	2.957	0.549	15	0.0324
sasd1011p_x3	0.305	2.743	0.348	14.7	0.0205
sasd1012i	0.061	0.671	0.049	13.4	0.014
sasd1013p	0.061	0.427	0.439	8.5	0.1315
sasd1015p	0.168	3.063	0.287	13.5	0.0309
sasd1017p	0.175	2.88	0.142	13.45	0.0145
sasd1022p	0.152	2.362	0.023	14.6	0.0025
sase005p_x1	0.152	1.981	0.13	14	0.0152
sase005p_x2	0.229	3.353	0.049	14.75	0.0037
sase006p	0.229	2.134	0.154	14.7	0.0121
sase022p	0.13	7.468	0.184	14.65	0.0256
sase1007p	0.168	4.42	0.206	14.85	0.022
sase1011i	0.091	0.457	0.058	18.3	0.011

Site ID	Channel Depth m	Channel Width m	Channel Velocity m s^{-1}	Temperature °C	Δ Temperature °C
sase1015i	0.152	0.853	0.012	14.5	0.0013
sase1018i	0.305	3.505	0.108	15	0.0063
sase1019i	0.335	6.096	0.003	15.1	0.0001
sase1020p	0.549	12.192	0.291	14.1	0.0095
sasv001p	0.122	0.686	0.047	13.95	0.0068
sasv010i	0.101	1.829	0.006	14.5	0.0008
sasv013i	0.091	4.572	0.003	14.7	0.0005
sasv019p	0.305	2.896	0.105	15.25	0.0061
sasw011_x2	0.076	1.524	0.006	14.6	0.0011
sasw011_x3	0.061	0.61	0.003	14.7	0.0007
sasw022	0.152	0.914	0.015	16	0.0017
sasw023p	3.048	25.908	0.148	15.8	0.0009
sira001i	0.122	1.981	0.053	14.05	0.0077
sira004p	0.396	9.144	0.306	16.95	0.0138
sirb010p	0.091	0.914	0.012	15.45	0.0021
sirb012p	0.991	11.43	0.123	17	0.0022
sirb1001e	0.061	0.823	0.009	15.5	0.0024
sird001p	0.503	12.04	0.293	12.65	0.0105
sird006e	0.204	4.572	0.006	11.4	0.0004
sird009p	0.168	1.067	0.052	12.2	0.0055
sird011i	0.091	0.762	0.018	13.4	0.0035
sird016p_x	0.229	3.048	0.072	12	0.0056
sird1005i	0.024	0.61	0.021	16.2	0.0147
sire001i	0.137	3.505	0.012	13.8	0.0014
sirv001p	0.213	2.438	0.168	16.3	0.014
sirw001	0.282	3.962	0.127	15.35	0.008
WDH-103	0.7	30.48	0.005	12.1	0.0001
WDH-104	0.07	3.353	0.005	16.45	0.0009
WDH-105	0.122	0.914	0.067	15	0.0097
WDH-18	0.107	1.372	0.117	14.95	0.0197

References

Dingman, S. (2003). Evapotranspiration. In S. L. Dingman, *Physical Hydrology* (3rd ed.).